BIOCHEMISTRY
including biophysical chemistry & molecular biology

ARTICLE

pubs.acs.org/biochemistry

Topology and Accessibility of the Transmembrane Helices and the Sensory Site in the Bifunctional Transporter DcuB of *Escherichia coli*

Julia Bauer,[‡] Max J. Fritsch,[§] Tracy Palmer,[§] and Gottfried Unden*[,‡]

[‡]Institute for Microbiology and Wine Research, Johannes Gutenberg-University, Becherweg 15, 55099 Mainz, Germany

[§]College of Life Sciences, Division of Molecular Microbiology, University of Dundee, Scotland

Supporting Information

ABSTRACT: C_4-Dicarboxylate uptake transporter B (DcuB) of *Escherichia coli* is a bifunctional transporter that catalyzes fumarate/succinate antiport and serves as a cosensor of the sensor kinase DcuS. Sites and domains of DcuB were analyzed for their topology relative to the cytoplasmic or periplasmic side of the membrane and their accessibility to the water space. For the topology studies, DcuB was fused at 33 sites to the reporter enzymes PhoA and LacZ that are only active when located in the periplasm or the cytoplasm, respectively. The ratios of the PhoA and LacZ activities suggested the presence of 10 or 11 hydrophilic loops, and 11 or 12 α-helical transmembrane domains (TMDs). The central part of DcuB allowed no clear topology prediction with LacZ/PhoA fusions. The sites of DcuB accessible to the hydrophilic thiol reagent 4-acetamido-4′-maleimidylstilbene-2,2′-disulfonate (AMS) were determined with variants of DcuB that carried single Cys residues. After intact cells were labeled with the membrane-impermeable AMS, denatured cells were differentially labeled with the thiol reagent polyethylene-glycol-maleimide (PEGmal) and analyzed for a mass shift. From 35 positions 17 were accessible to AMS in intact bacteria. The model derived from topology and accessibility suggests 12 TMDs for DcuB and a waterfilled cavity in its central part. The cavity ends with a cytoplasmic lid accessible to AMS from the periplasmic side. The sensory domain of DcuB is composed of cytoplasmic loop XI/XII and a membrane integral region with the regulatory residues Thr396/Asp398 and Lys353.

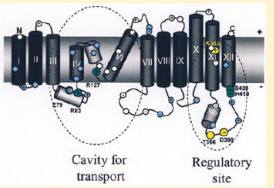

The C_4-dicarboxylates play an important role in carbon metabolism of *Escherichia coli* under aerobic and anaerobic conditions when no hexoses or related compounds are available. Under anaerobic conditions C_4-dicarboxylates such as fumarate, L-malate, and aspartate are used as electron acceptors in the fumarate respiration pathway (for review, see refs 1−3). The C_4-dicarboxylates are taken up into the cell, converted to fumarate, and reduced to succinate. Succinate cannot be further metabolized by *E. coli* under anaerobic conditions and is excreted. Uptake of the C_4-dicarboxylates and excretion of succinate is mediated by DcuB that catalyzes an electroneutral C_4-dicarboxylate/succinate antiport.[3−5] DcuB is produced under anaerobic conditions in the presence of C_4-dicarboxylates.[6−8] The homologue DcuA is an alternative transporter of the Dcu family and is able to partially substitute for DcuB in *dcuB* deletion mutants.[4,9,10] DcuA is constitutively produced and catalyzes C_4-dicarboxylate/succinate antiport similar to DcuB. The physiological role of DcuA is not clear, but it was suggested to supply *E. coli* under aerobic and anaerobic conditions with C_4-dicarboxylates as the C-source. A third transporter, DcuC, is also able to replace DcuB in C_4-dicarboxylate/succinate antiport.[9,11] The physiological role of DcuC is succinate export during glucose fermentation. DcuC has low similarity to DcuB and DcuA and constitutes a new family of secondary C_4-dicarboxylate transporters (DcuC family).

DcuB functions as a cosensor of the DcuS-DcuR two-component system sensor kinase DcuS.[12−14] DcuS-DcuR induces the genes of fumarate respiration and aerobic C_4-dicarboxylate uptake in the presence of extracellular C_4-dicarboxylates.[6,8,14] The DcuS-dependent genes of fumarate respiration include *dcuB*, *fumB*, and the *frdABCD* genes encoding DcuB, fumarase FumB, and fumarate reductase FrdABCD. The expression of *dcuB* depends on a functional DcuS-DcuR system. In addition, the gene expression is subject to anaerobic induction by the transcriptional regulator FNR. DcuS contains a periplasmic PAS domain (PAS_P) that binds C_4-dicarboxylates.[13,15,16] The domain is linked by two transmembrane helices to the membrane and the cytoplasmic domains. Thus, DcuS has the typical composition of a periplasmic sensing His kinase[17,18] with an extracellular sensing domain for hydrophilic stimuli. Despite the presence of an effector binding domain,[13−16] DcuS requires DcuB as a cosensor during anaerobic growth.[12] DcuS is permanently active in the absence of DcuB, suggesting that DcuB is required to silence DcuS in the absence of C_4-dicarboxylates. Of the Dcu transporters, only DcuB has a regulatory function, and DcuA and DcuC are inactive in cosensing.[12]

Point mutations of DcuB (K353A, T394I, and D398N) were identified that abolish the function of DcuB as a cosensor while retaining the transport function.[12] Two of the amino acid residues (T394 and D398) are located in hydrophilic loops close to the N-terminal end of DcuB or in a transmembrane helix, depending on the prediction program. The third residue (K353) is found in a predicted TMD. Transport specific sites are located

Received: December 16, 2010
Revised: June 1, 2011
Published: June 02, 2011

close to the center of the protein sequence, demonstrating that DcuB is a bifunctional protein with separate transport and regulatory sites. It is not known how DcuB controls the function of DcuS. The same applies to other membrane-integral sensor/cosensor pairs where neither the mode of signal transfer nor the interacting domains of the sensors and of the cosensors are known.[19]

DcuB is predicted to consist of 10−12 TM helices depending on the prediction algorithm. The topology predictions vary in particular for the C-terminal part of the protein which contains the sensory domain. Therefore, the location and topology of the sensory domain with respect to the membrane are unknown. To understand the role of DcuB in sensing and its interaction with DcuS, the topology and location of sensory sites and of DcuB in general need to be defined.

Overproduction of DcuB inhibits bacterial growth, and treatment of membranes with detergent yields no significant amounts of solubilized or purified DcuB. Therefore, DcuB was analyzed in vivo for its transmembrane topology, the number of TM helices and hydrophilic loops. For these studies, C-terminal fusions of DcuB to β-galactosidase or alkaline phosphatase were used.[20] β-Galactosidase and alkaline phosphatase only show activity when located in the cytoplasm or in the periplasm of *E. coli*, respectively. In this way, a model for the topology of TM helices and hydrophilic loops was generated, which was subsequently tested and refined by studies on the accessibility of specific DcuB sites from the periplasmic water space. The accessibility was studied with the membrane impermeant labeling reagent 4-acetamido-4′-maleimidylstilbene-2,2′-disulfonate (AMS) in recombinant forms of DcuB carrying single Cys residues at specific sites.[21,22] The β-galactosidase/alkaline phosphatase fusion experiments together with AMS accessibility studies gave a consistent model for DcuB topology and location of functional sites. Results show that DcuB differs significantly in topology and arrangement of TM helices from the closely related DcuA.[23]

EXPERIMENTAL PROCEDURES

Bacteria, Plasmids, Molecular Genetic Methods. *Escherichia coli* K-12 strains and plasmids used in this study are listed in Table 1. Molecular genetic methods were performed according to standard procedures.[24] Growth was performed in Luria−Bertani (LB) broth for all genetic experiments. Plasmid DNA, PCR products, and restriction fragments were isolated and purified using kits (Qiagen, Hilden). Restriction endonucleases and T4 DNA ligase were obtained from MBI Fermentas. *E. coli* strains were transformed by electroporation[25] or heatshock. For generation of plasmid-encoded point mutants, the QuikChange Site-Directed Mutagenesis kit (Stratagene, La Jolla, USA) was used, or *Pfu*Ultra (Stratagene) in combination with *Dpn*I endonuclease (Fermentas), and heatshock-competent JM109 cells. Oligonucleotides were from Eurofins and Sigma Aldrich.

Cultivation of Bacteria. For growth experiments *E. coli* was cultivated under anaerobic conditions in enriched M9 (eM9) medium[26] with acid-hydrolyzed casamino acids (0.1%) and tryptophan (0.0005%), supplemented with glycerol (50 mM) and disodium fumarate (50 mM). For anaerobic expression studies (determination of chromosomally encoded β-galactosidase activity) and transport measurements, cells were grown anaerobically in the same medium supplemented with 50 mM DMSO. Growth for activity measurement of DcuB-LacZ or DcuB-PhoA fusion strains (plasmid located *dcuB-lacZ* or *dcuB-phoA* fusions) and for labeling of DcuB-PhoA was performed in LB broth with 50 mM sodium fumarate under aerobic conditions. All media were inoculated with 1−5% (v/v) of an overnight culture grown under the same conditions and cultivated at 37 °C. If appropriate, antibiotics were added as follows: 100 μg mL^{-1} ampicillin, 50 μg mL^{-1} kanamycin, 50 μg mL^{-1} spectinomycine, 20 μg mL^{-1} chloramphenicol, and 15 μg mL^{-1} tetracycline. When two or more antibiotics were supplied simultaneously, half of the concentrations were used.

Construction of *dcuB* Encoding Plasmids. Two sets of *dcuB* coding plasmids were used for the experiments. First, for functional studies, for example, analysis of the sensory function of DcuB, transport studies with wild-type DcuB and the different Cys-substituted variants, and for growth experiments, plasmid pMW228 and derivatives, were used (Table 1, and Supplementary Table S1, Supporting Information for the full list of plasmids). Plasmid pMW228 is present in low copy number (pME6010 derivative) and codes for a full-length *dcuB* gene under the control of its own promoter. Second, the genes coding for DcuB-LacZ and DcuB-PhoA fusion proteins, and for the cysteine variants for labeling experiments were carried on derivatives of pBAD18-Kan[27] under the control of the arabinose-inducible pBAD promoter.

Because of the lack of a ribosome binding site (RBS) in the pBAD vectors, the *dcuB* gene was amplified from pMW228 using primers dcuB-3+-*Eco*RI2 5′-GGTTCACACATGGAATTCACTATC-3′ and dcuB-3+-XhoI2 5′-CATTTACTCGAGCCCGTACATC-3′ and cloned first into vector pASK-IBA3$^+$. By using the restriction sites *Xba*I and *Hind*III, the gene including the RBS sequence of pASK-IBA3$^+$ was then inserted into the pBAD18-Kan vector resulting in plasmid pMW445 (coding for DcuB(3−444) with a C-terminal Streptag). For the topology studies with DcuB-LacZ, the *lacZ* gene was amplified from the plasmid pT7−5-putP-lacZ[28] by PCR with the primers lacpho2-*Pst*I-for and lacZ2-rev. The *Pst*I and *Hind*III digested PCR product was cloned into pMW445 to obtain pMW560 coding for MGDRGPE-DcuB(3−444)-LEVDLQESAS-LacZ(10−1024). For the other DcuB-LacZ fusions with C-terminally truncated DcuB, 3′-truncated fragments of *dcuB* were amplified from pMW445 with pBAD-dcuBXbaIfor in combination with the dcuB-*Pst*I-re primer set (Supplementary Table S2, Supporting Information) and cloned into pMW560. For DcuB-PhoA (*dcuB-phoA*) fusions for the topology (or PhoA activity) studies, the *phoA* gene was amplified from plasmid pT7−5-putP-phoA[28] using primers lacpho2-*Pst*I-for and phoA2-*Hind*III-re. The PCR fragment was inserted into pMW445 by the flanking *Pst*I and *Hind*III restriction sites. The resulting plasmid pMW561 codes for MGDRGPE-DcuB(3−444)-LEVDLQESASDSYTQVASWTEPFPFC-PhoA(27−471), hereafter referred to as DcuB-PhoA. N-terminal fragments of DcuB in DcuB-PhoA were obtained by amplification of the *dcuB′* gene from pMW445 with pBAD-dcuBXbaIfor and a series of dcuB-*Pst*I-re primers. The PCR-produkts were ligated with XbaI- and *Pst*I-restricted and dephosphorylated pMW561 resulting in pMW561 derivatives coding for fusions of C-terminally truncated DcuB with PhoA.

For growth, transport measurements and sulphydryl-labeling, single and multiple cysteine variants of DcuB and DcuB-PhoA were generated by site-directed mutagenesis of the initial plasmids pMW228 and pMW561. First, the five cysteine residues of DcuB were replaced step by step by serine residues using

Table 1. Strains and Plasmids

E. coli K12 strains		genotype	reference or source
C43(DE3)		strain for overexpression of membrane proteins carrying a chromosomal T7 polymerase	56
CC181		*F128lacIq* Δ(*ara,leu*)*7679* Δ*lacX74* Δ*phoA20 galE galK thi rpsE rpoB argEam lacY328am recA1*	30
MC4100		F$^-$ *araD139* Δ(*argF-lac*)*U169, rpsL150, (*Δ*lacZ), relA1 flbB530 deoC1 ptsF25 rbsR*	57
IMW505		MC4100 but λ (Φ *dcuB*$^-$*lacZ*) *dcuA::Spec*^{r} Δ*dcuB dcuC::Cam*^{r}	12
plasmids		**genotype**	**reference or source**
pBAD18-Kan		expression vector; pBR322 *ori*, arabinose-inducible P_{BAD} promoter, *Kan*^{r}	27
pME6010		low-copy plasmid, *Tet*^{r}	58
pASK-IBA3$^+$		vector for protein expression with C-terminal streptagII, AHT-inducible; *Amp*^{r}	IBA, Göttingen
pT7−5-putP-lacZ		plasmid for expression of *putP-lacZ*; source for *lacZ* (AA10), *Amp*^{r}	28
pT7−5-putP-phoA		plasmid for expression of *putP-phoA*; source for *phoA* without export signal (AA27), *Amp*^{r}	28
pHASoxYZ		plasmid for constitutive expression of *HA-soxY* and *soxZ* from *Paracoccus pantotrophus*, *Cam*^{r}	Fritsch and Palmer, unpublished
		dcuB Plasmids	
pMW228		*dcuB EcoRI-Xho*I with own promoter in pME6010, *Tet*^{r}	12
pMW445		*dcuB Xba*I-*Hind*III with C-terminal Streptag in pBAD18-Kan, 6871 bp, *Kan*^{r}	this study
pMW560		*lacZ Pst*I-*Hind*III in pMW445 for expression of *dcuB-lacZ*; 9886 bp, *Kan*^{r}	this study
		template for a series of truncated *dcuB-lacZ* constructs (see Table S1)	
pMW561		*phoA* (without export signal) *Pst*I-*Hind*III in pMW445 for expression of *dcuB-phoA*; 8275 bps, *Kan*^{r}	this study
		template for a series of truncated *dcuB-phoA* constructs (see Table S1)	
pMW462	**C_1S**	pMW228 but *dcuB* C13S	this study
pMW463	**$C_{2,3}$S**	pMW228 but *dcuB* C98S and C104S	this study
pMW464	**C_4S**	pMW228 but *dcuB* C387S	this study
pMW465	**C_5S**	pMW228 but *dcuB* C433S	this study
pMW735	**$C_{4,5}$S**	pMW228 but *dcuB* C387S and C433S	this study
pMW736	**$C_{2,3,4,5}$S**	pMW228 but *dcuB* C98S, C104S, C387S and C433S	this study
pMW788	**$C_{1,2,3,5}$S**	pMW228 but *dcuB* C13S, C98S, C104S and C433S	this study
pMW737	**$C_{1,2,3,4,5}$S**	pMW228 but *dcuB* C13S, C98S, C104S, C387S and C433S	this study
pMW826	**DcuB*- PhoA**	pMW561 but *dcuB* 5-fold mutant: C13S, C98S, C104S, C387S, C433S plus C(linker)S	this study
pMW911		pMW826 but *phoA* C168S, C286S and C336S	this study
pMW912		pMW826 but *phoA* C168S, C178S and C336S	this study
pMW828	**DcuB*- PhoA***	pMW826 but *phoA* C168S, C178S; C286S and C336S	this study
		dcuA Plasmids	
pMW565		pMW560 but *dcuA Xba*I-*Xho*I instead of *dcuB* for expression of a DcuA-LacZ fusion protein;	this study
		template for a series of truncated *dcuA-lacZ* constructs (see Table S1)	
pMW577		pMW561 but *dcuA Xba*I-*Xho*I instead of *dcuB* for expression of a DcuA-PhoA fusion protein;	this study
		template for a series of truncated *dcuA-phoA* constructs (see Table S1)	

complementary mutagenesis primer pairs dcuB-Cys1mut-for/ -rev, dcuB-Cys2mut-for/ -rev (for simultaneously exchange of C2S and C3S), dcuB-Cys4mut-for/ -rev and dcuB-Cys5mut-for/ -rev. Additionally, the four cysteine residues of PhoA and the cysteine residue in the DcuB-PhoA linker region were replaced by Ser residues in *dcuB-phoA* of pMW561, using primers PhoA-C1S-for/ -rev, PhoA-C2S-for/ -rev PhoA-C3S-for/ -rev PhoA-C4S-for/ -rev and C-linker-PhoA-for/ -rev. Plasmids pMW737 (pMW228 derivative) and pMW828 (pMW561 derivative) for the expression of Cys-less DcuB (DcuB*) and DcuB-PhoA (DcuB*-PhoA*) were used as templates for single cysteine-replacements on positions of interest (see Supplementary Table S1, Supporting Information).

Construction of *dcuA* Encoding Plasmids. The construction started from pBAD18-Kan derived plasmid pMW565 and pMW577 encoding DcuA-PhoA and DcuA-LacZ fusion proteins (MGDRGPEF-DcuA-(2−433)-EVDLQESASDSYTQVASWTEP-FPFC-PhoA(27−471)) and (MGDRGPEF-DcuA(2−433)-EVD-LQESAS-LacZ(10−1024)). The expression plasmids are identical to pMW560 and pMW561 but contain *dcuA* instead of *dcuB*. C-terminally truncated *dcuA* fragments were amplified with pBAD-dcuBXbaIfor and different dcuA-XhoI-re primers (Supplementary Tables S2 and S3, Supporting Information) and cloned into restricted and dephosphorylated pMW565 and pMW577 replacing the full-length *dcuA* gene (Table 1, and Supplementary Table S1, Supporting Information).

Enzyme and Transport Assays. Alkaline phosphatase (PhoA)[29,30] and β-galactosidase (LacZ)[31] activities were measured colorimetrically by the hydrolysis of PNPP or ONPG, respectively, in permeabilized bacteria of strain CC181 with plasmid located *dcuB-phoA* or *dcuB-lacZ* fusions of pMW561

dx.doi.org/10.1021/bi1019995 |*Biochemistry* 2011, 50, 5925–5938

and pMW560 and derivatives. The bacteria were grown in LB broth with or without 50 mM disodium fumarate (which gave the same result) at 37 °C under aerobic conditions. In the exponential growth phase, the cells were induced with 0.2% (13.3 mM) arabinose and cultivated for 3 h at 30 °C. For expression studies with chromosomally located *dcuB-lacZ*, cells were grown anaerobically in eM9 medium supplemented with glycerol, DMSO, with or without fumarate to the exponential growth phase ($OD_{578\ nm}$ of 0.5−0.8) at 37 °C. For each strain and condition, at least two independent cultures were grown and enzyme activities of each culture were determined in quadruplicate. For transport assays, uptake of [^{14}C]succinate was determined in anaerobically grown bacteria as described previously.[12]

Labeling and Detection of DcuB-PhoA. Labeling by AMS, *N*-ethylmaleimide (NEM), and polyethylene-glycol-maleimide (PEGmal) was performed with *E. coli* C43DE3 expressing a single-cysteine variant of DcuB*-PhoA* (pMW828 derivative) in combination with HA-SoxY (pHASoxYZ). Antisera raised against the long cytoplasmic loop of DcuB ($DcuB_{W194-Q207}$) showed only very weak reaction with full-length DcuB. Strep-tagged DcuB showed no reaction with Strep-tag antibodies, and His-tagged DcuB (C- and N-terminal) was not functional. Therefore, DcuB-PhoA was used for the accessibility experiments, using the PhoA protein as an epitope for immunodetection with anti-PhoA antisera. For the reaction with anti-PhoA, cells were grown aerobically in LB broth plus 50 mM sodium fumarate until the mid-exponential growth phase and expression was induced with 0.2% (13.3 mM) arabinose for 4 h at 30 °C. Additionally, 20 mM potassium phosphate pH 6.8 was added to prevent the expression of chromosomally encoded alkaline phosphatase. Cells were harvested by centrifugation (5000*g*, 10 min, 4 °C), washed twice with HEPES/NaCl buffer (50 mM HEPES, 250 mM NaCl, pH 6.8), and resuspended in HEPES buffer (50 mM HEPES, 50 mM NaCl, pH 6.8) to a total cell protein concentration of 10 μg/μL.

The maleimides NEM and PEGmal were freshly dissolved in HEPES buffer to yield 50 mM stock solutions, whereas a 20 mM stock solution of AMS in HEPES buffer was stored in aliquots at −80 °C protected from light. For labeling 10 μL cell suspension (100 μg of total cell protein) were supplied with HEPES buffer and labeling reagent as indicated to a reaction mixture with a total volume of 50 μL. For each cell suspension, four different labeling reactions were run: sample (AP), (NP), (P), and (−). Samples (AP) and (NP) were labeled in two consecutive steps by AMS and PEGmal, or NEM and PEGmal, respectively. All labeling reactions were performed for 1 h to ensure reaction of all accessible residues with the maleimide derivatives. Control experiments showed that maximal labeling was achieved after 5 min for NEM and 15 min for AMS. For sample AP the washed cells were incubated in the first step with 2 mM AMS, sample (NP) with 2 mM NEM, and samples (P) and (−) without any labeling reagent. The labeling reactions were conducted at room temperature with occasional vortexing and stopped by 20-fold dilution with HEPES buffer followed immediately by centrifugation. The cell pellets were washed with HEPES buffer and the supernatants were carefully removed using a pipet tip. The cell pellets were resuspended in 45 μL of HEPES buffer containing 1.3% SDS and samples (AP), (NP), and (P) where mixed with 2 mM PEGmal. The samples were incubated for 1 h with the PEGmal, and the reactions were terminated by adding 5 μL of 0.5 M dithiothreitol. The protein samples were immediately mixed with SDS loading buffer, boiled for 10 min, subjected to SDS-PAGE, and subsequently transferred to a nitrocellulose membrane (Protran, Schleicher & Schuell or Amersham Hybond-ECL). The blotted proteins were analyzed for HA-SoxY and DcuB-PhoA by a solution containing anti-HA (detection of HA-SoxY) and anti-PhoA (detection of DcuB-PhoA) antibodies, and for assay the Millipore Immobilon Western Chemiluminescent HRP Substrate (Millipore) was used. The primary antibodies were mouse Monoclonal Anti-PhoA (Sigma; dilution 1:20000) and Monoclonal Anti-HA, coupled to horseradish peroxidase HRP (Sigma, dilution 1:20000). The secondary antibodies were rabbit anti-IgG, coupled to HRP (Bio-RAD, dilution 1:10000) and mouse anti-IgG, coupled to HRP (Qiagen, dilution 1:10000). Chemoluminescence was detected after exposure to a film sheet and development (Immobilon Western Chemiluminescent HRP, Millipore).

RESULTS

The Hydrophilic Loop Topology of DcuB Analyzed by PhoA and LacZ Fusions. In vitro studies with DcuB are prevented by the toxicity of DcuB upon overproduction, the very poor solubility of DcuB in detergent, and poor binding of tagged forms to affinity columns (Bauer and Unden, unpublished results). Therefore, in vivo methods were used for topology and accessibility studies of DcuB that were performed under conditions of moderate expression of *dcuB*. For topology studies, the 3′-truncated forms of *dcuB* gene were fused with their 3′-end to *lacZ* and *phoA* genes encoding β-galactosidase (LacZ) or alkaline phosphatase (PhoA), respectively. In this way, C-terminally truncated forms of DcuB were obtained that are fused with their C-terminus to intact LacZ or PhoA enzymes. The fusions were produced at positions in or close to predicted periplasmic or cytoplasmic loops of DcuB (Figure 1). Overall, fusions to PhoA and LacZ were produced at 33 sites, starting at DcuB(R19) and ending at DcuB(G444). For fusions DcuB(R19) and DcuB(G22) membrane integration was confirmed by differential centrifugation of membrane fractions. The constructs were encoded on plasmid pBAD to allow moderate expression after induction, and the activities of PhoA and LacZ were tested after growth under inducing conditions. The activities of the fusions varied in an inverse mode for both enzymes depending on the fusion site (Figure 2). Topologies of the fusion sites were derived from the ratio of the PhoA/LacZ activities and the progression of changes relative to neighboring fusion sites. In addition, the topologies obtained in this way were related to the topology predicted by the TMHMM server. By combining the information, 12 TMDs are suggested (Figure 2).

The fusions of LacZ/PhoA at DcuB(R19) and DcuB(G22) that are located in the first supposed periplasmic loop showed very high activity for LacZ (up to 6000 U) and PhoA (up to 1400 U). The LacZ/PhoA ratio > 1 suggests a cytoplasmic location of the loop, but the topology is not clear from this data alone. However, the fusions showed stable localization in the membrane fraction after differential centrifugation of a cell homogenate (not shown), suggesting membrane integration of the fusion proteins and presence of a stable TMD in front of the R19/G21 loop. The fusions in the following hydrophilic loop at DcuB(L53) showed very high PhoA and low LacZ activity, which is a clear indication for a periplasmic location. This finding supports also the cytoplasmic topology of DcuB(R19) and DcuB(G22), since the R19/G21 and L53 loops are separated

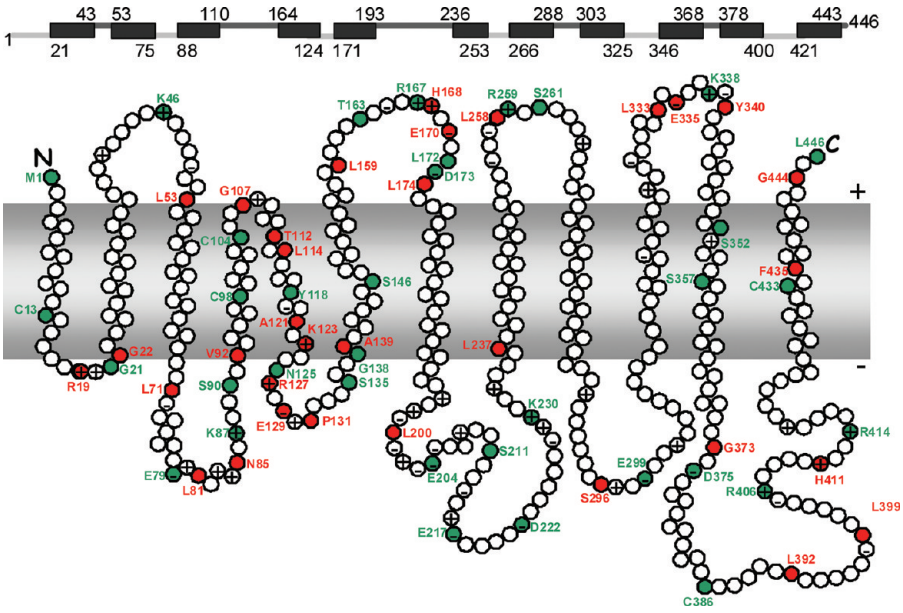

Figure 1. Prediction of TM helices of DcuB by the TMHMM algorithm (top panel) and topology model (bottom panel) of DcuB (12 TDM model) showing positions of DcuB-LacZ/PhoA fusions and sites for single Cys substitutions. The model is based on TMHMM prediction,[55] secondary structure prediction PSIPRED,[54] and the experimental data from the present study. The labeled positions show sites for LacZ or PhoA fusions (red), sites for single Cys substitutions (green), and the positions of basic (His, Lys, Arg, +) and acidic (Asp, Glu, −) amino acid residues. + and − indicate the periplasmic and cytoplasmic sides of the membrane.

by a TMD uniformly predicted by topology progams. The fusions to the third predicted loop (residues L71−V92) gave a very high LacZ/PhoA ratio of activities predicting cytoplasmic location of the L71/V92 loop. For the region following the third loop (G107−L159) that includes three predicted TMDs and two short loops, the ratio of activities was intermediate and allowed no clear identification of loop regions. For the subsequent region (residues H168−L174), the ratio of the PhoA/LacZ activities was high and characteristic for a periplasmic location of that loop. For the residual protein from residues 168 to 444, seven hydrophilic loops (separated by six TMDs) were suggested by the PhoA/LacZ ratios and the corresponding topology predictions. In this region, only the activities for residue F435 that has a predicted location within the membrane gave no clear indication for the topology.

In Figure 2B, the activity ratio of PhoA/LacZ is plotted against the sequence shown as a log presentation to present the ratios on a linear scale. Ratios > 1 (corresponding to 0 in the log scale) indicate an excess of PhoA activity and periplasmic location of the site, and a ratio < 1 indicates an excess of LacZ activity and cytoplasmic location of the site (Figure 2A). The sites in Figure 2B where the graph crosses from the positive to the negative side and vice versa represent the positions for TMDs and are indicated by arrows (which give only the location of the TMDs, but the distances are not drawn to scale). Overall, the PhoA/LacZ ratios gave experimental support for the presence of 12 TMDs that are separated by 11 hydrophilic loops on alternating sides of the membrane, and for a periplasmic location of the N- and C-terminal ends of DcuB (Figures 1 and S1). Fusions with high positive or negative log values for the activity ratios are highly predictive for periplasmic and cytoplasmic location. On the other hand, log values in the range from +0.2 to −0.2 suggest no clear or stable preference for periplasmic or cytoplasmic location of the site as suggested by comparing topology prediction and experimental testing. This could be due to a membrane integral location of the site or of a labile secondary structure at the respective position. The activity ratios, however, gave no clear indication for the number and location of hydrophilic loops and TM helices in the region between residues 107 and 159, and the suggested TM helices had varying locations in different prediction programs.

Comparative Analysis of the DcuA Topology by PhoA and LacZ Fusions. Earlier, the topology of the transporter DcuA was shown by using β-lactamase (BlaM) fusions to consist of 10 TM helices.[23] To confirm the significant differences in topology of the closely related DcuA and DcuB transporters that are members of the Dcu family,[3] the topology of DcuA was studied by the use of LacZ and PhoA fusions as for DcuB to exclude methodical differences. The topology derived from the PhoA and LacZ fusions (Figure S1, Supporting Information) corresponds to the BlaM-derived topology of DcuA with 10 TM helices and periplasmic location of the N- and C-terminal ends of DcuA.[23]

The Cys Residues of DcuB Are Not Essential for Its Function. To further probe the topology of DcuB, the accessibility of single Cys residues to hydrophilic and hydrophobic reagents was tested. For this purpose, variants of DcuB were produced containing Cys residues at distinct sites (Figure 1). The variants were derived from a Cys-less variant of DcuB (DcuB*) as a starting material that is not labeled by thiol reagents. In DcuB* the native Cys residues (C13, C98, C104, C386, and C433) were replaced by Ser residues. The Cys-variants, including the Cys-less DcuB*, were tested for their functionality in anaerobic growth, in fumarate transport, and in the regulatory activity (control of DcuS). The DcuB variants were encoded on the low copy plasmid pMW228 under control of the native *dcuB* promoter. For testing function, the variants were produced in a *dcuA dcuB dcuC* mutant strain where anaerobic growth on glycerol plus fumarate depends on a functional DcuB protein.[3,11] For reasons of simplicity, the Cys → Ser replacement mutants for construction of the Cys-less mutant

dx.doi.org/10.1021/bi1019995 |*Biochemistry* 2011, 50, 5925–5938

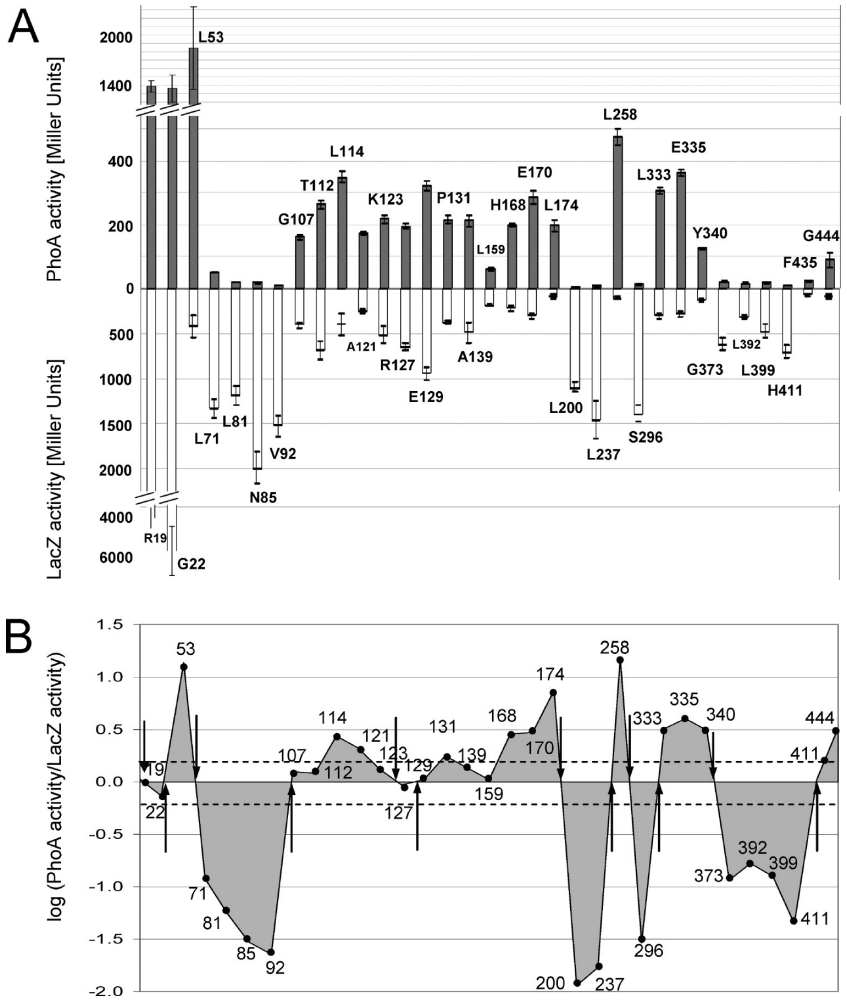

Figure 2. Alkaline phosphatase (PhoA) and β-galactosidase (LacZ) activities of DcuB-PhoA and DcuB-LacZ protein fusions (A) and PhoA/LacZ activity ratios (B). Plasmid-borne *dcuB-phoA* (plasmid pMW561 and derivatives) and *dcuB-lacZ* (plasmid pMW560 and derivatives) fusions encoding DcuB-PhoA or DcuB-LacZ were expressed in *E. coli* CC181 under the control of the P_{BAD} promoter. Cells were grown aerobically in LB broth and production of the fusion proteins was induced with 0.2% arabinose in the exponential growth phase for 3 h. (A) Alkaline phosphatase and ss-galactosidase activity was determined by measuring the rate of PNPP or ONPG hydrolysis, respectively. The amino acid residues indicate the last amino acid residue of DcuB at the fusion site with PhoA or LacZ. (B) The ratio of PhoA/LacZ activities was calculated from the normalized activities (% activity of the maximal activities (1845 MU of $DcuB_{L53}$-PhoA, and 5766 MU of $DcuB_{G22}$-LacZ)). Log_{10} of the ratio is shown. The sites correspond to the fusions given in A). The sites for TMDs predicted from the activity ratio and graph progression are indicated by arrows. The broken lines gives the threshold (log PhoA/LacZ = $\pm$ 0.2) for clear-cut periplasmic or cytoplasmic location of the site (see text).

were termed DcuB(C_1S) or DcuB($C_{1,2}$S) and so on. Single, double, or triple Cys → Ser variants of DcuB, lacking the Cys residues in various combinations, grew like the wild-type on glycerol plus fumarate (Table 2). Only the 4- and the 5-fold Cys variants lacking Cys386 as one of the Cys residues were decreased in growth rate by a factor of approximately 2. The transport rates for fumarate uptake decreased in the 5-fold variant also by a factor of 2, whereas double, triple, and some of the 4-fold Cys variants of DcuB were not significantly affected (Table 2). Multiple Cys → Ser variants that were decreased in growth and transport activity generally included the Cys386Ser substitution. Strains harboring multiply substituted proteins with Cys386 in the wild-type state like DcuB($C_{1,2,3,5}$S) were not impaired in growth and transport. Nevertheless, Cys386 is not essential, and some DcuB proteins with a Cys386 → Ser replacement, like DcuB($C_{4,5}$S), were fully active (Table 2).

The regulatory capacity of DcuB and of the Cys replacement variants was tested by measuring the expression of chromosomal *dcuB-lacZ*. DcuB inhibits the DcuS target gene expression in the absence of fumarate.[12] Strains with wild-type DcuB show a fumarate-dependent induction by a factor of 18 $\pm$ 6 ("control factor", Table 2), whereas *dcuB* deletion or regulatory mutations (e.g., DcuB(T394I)) were fully induced in the absence of fumarate (Table 2) as described earlier. None of the single or multiple Cys mutants lost the capacity for fumarate-dependent regulation of DcuS.

Overall, the Cys 5-fold and the other Cys variants of DcuB were active with respect to growth, transport, and its regulatory function, demonstrating that the DcuB Cys-less (or DcuB*) protein can be used for studies on function and accessibility.

Accessibility of Cys Residues in DcuB by Differential Labeling with AMS/NEM and PEGmal. Sites of DcuB accessible to molecules with polar groups from the outside of the cell were identified by a two-step labeling procedure using AMS or NEM in a first step in intact cells, and PEGmal in the second step.

dx.doi.org/10.1021/bi1019995 |*Biochemistry* 2011, 50, 5925–5938

Table 2. Effect of DcuB Variants on Anaerobic Growth on Glycerol Plus Fumarate, Fumarate Uptake and DcuB Dependent Regulation (Repression of DcuS Function)[a]

DcuB	growth on Glyc + Fum	fumarate uptake (U/g dw)	*dcuB-lacZ* (Miller U)		
			−Fum	+Fum	+Fum/−Fum
Strains with DcuB-derivatives on pME6010					
DcuB (wild-type)	+++	9.2 ± 1.2	17 ± 1	405 ± 19	23.8
DcuB- (Δ*dcuB*)	−	1.8 ± 0.4	460 ± 22	415 ± 25	0.9
DcuB-PhoA[b]	++(+)	n.d.	n.d.	n.d.	n.d
DcuB(C_4S)	+++	n.d.	11 ± 1	308 ± 5	28
DcuB($C_{4,5}$S)	+++	7.0 ± 1.3	9 ± 1	333 ± 23	37
DcuB($C_{1,2,3}$S)	+++	8.5 ± 2.0	10 ± 2	356 ± 18	36
DcuB($C_{1,2,3,5}$S)	+++	9.2 ± 1.6	13 ± 1	417 ± 27	32
DcuB($C_{2,3,4,5}$S)	++(+)	4.7 ± 0.9	23 ± 2	412 ± 14	17.9
DcuB($C_{1,2,3,4,5}$S) ≡ DcuB*	+(+)	4.7 ± 0.6	16 ± 2	414 ± 54	25.9
Strains with DcuB-derivatives on pBAD18					
DcuB (wild-type)	+++	n.d.	8 ± 2	255 ± 16	31.9
DcuB-PhoA	++(+)	n.d.	9 ± 1	250 ± 16	27.8
DcuB*-PhoA*	−	n.d.	48 ± 10	225 ± 52	4.7
DcuB*	−	n.d.	48 ± 10	166 ± 33	3.5

[a] Anaerobic growth was tested in eM9 medium supplemented with glycerol plus fumarate (50 mM each). Growth rate (high +++ to low +; no growth −) was derived from from growth curves. Uptake of [^{14}C]fumarate was measured as described in cell suspensions of *E. coli* IMW505 grown anaerobically on glycerol plus fumarate; DcuB and its variants were produced from plasmids of the pME6010 series (see Table 1 and Supplementary Table 1). For determining the control of *dcuB-lacZ*, the expression of the chromosomal *dcuB-lacZ* reporter gene fusion was determined (Miller U) in *E. coli* IMW505. For the expression studies, the bacteria were grown on glycerol plus DMSO in eM9 medium under anaerobic conditions to $OD_{578\ nm}$ = 0.5 to 0.8. The control factor gives the ratio of expression (β-galactosidase activities) after growth with and without fumarate induction as described by Kleefeld et al.[12] For the DcuB Cys → Ser single replacements DcuB(C_4S) is given; the other single replacements DcuB(C_1S), DcuB(C_2S), DcuB(C_3S), or DcuB(C_5S) showed similar behaviour in transport and regulatory competence. +++ to + stands for high to low growth rate, − for lack of significant growth. n.d., not determined. [b] Derivative of pMW561.

Labeling by PEGmal was performed after dissolving membranes and proteins by SDS to disclose Cys residues that were not previously labeled by AMS or NEM. Labeling of the Cys residues by AMS and NEM, respectively, was used to differentiate between the access and reactivity of thiol groups to a hydrophilic and a lipophilic reagent. Generally, reaction with NEM can be used as a reference for 100% blocking of a residue. Only Cys residues in a highly hydrophobic environment that are not able to release the proton to produce a thiolate are not able to react with NEM.[32,33]

Overall, 39 Cys-less (or DcuB*) variants of DcuB with single Cys substitutions at different positions were tested, 37 of these gave reproducible results. Each variant was analyzed in up to four independent experiments to obtain clear-cut results. The variants contained a C-terminal fusion of PhoA that allowed specific and highly sensitive detection of the protein with anti-PhoA antisera. The DcuB-PhoA fusion was fully active in growth and regulatory function of DcuB (Table 1). In the PhoA-tag, the four Cys residues of wild-type PhoA were replaced by Ser residues in order to obtain a variant (PhoA*) not interfering with Cys labeling in DcuB* mutants. DcuB*-PhoA* as well as DcuB-PhoA showed high and specific response to anti-PhoA antisera in immonoblotting.

Different types of responses to the differential labeling are shown in Figure 3. In the first example, intact bacteria containing DcuB*-PhoA* with single Cys residues were incubated with either AMS or NEM, followed by PEGmal after SDS treatment. Generally, AMS is not able to penetrate intact membranes and has access only to Cys residues that are located on the periplasmic side of the membrane, or in cavities on the periplasmic side accessible to the water space. NEM on the other hand is able to penetrate the membrane and to access lipophilic and hydrophilic space. Incorporation of PEGmal was monitored by the decrease of mobility by about 20 kDa after SDS-PAGE and immunoblotting with anti-PhoA serum. The mass increase allowed differentiation of DcuB-PEGmal from DcuB, DcuB-AMS, or DcuB-NEM. Labeling by AMS (540 Da) or NEM (125 Da) alone caused no observable mass shift and was detected only indirectly by the second labeling step. In addition, two control samples were prepared where the bacteria were denatured by SDS without PEGmal treatment (0% labeling) or treated with SDS and then with PEGmal without prior reaction with AMS or NEM (full PEGmal labeling). The labeling is shown in Figure 3 for a NEM (DcuB*(S98C)-PhoA*) and an AMS (DcuB*(R167C)-PhoA*) accessible residue for all conditions.

The intactness of the cells and the suitability of the system were tested by measuring the accessibility of Cys residues in a heterologously produced SoxY protein with ascertained cytoplasmic location, and of DcuB*-PhoA*(S286C), where PhoA* has an assured periplasmic location. A cytoplasmic version of SoxY is coproduced with the DcuB*-PhoA* proteins and contains one reactive Cys residue. SoxY serves as an internal reference for accessibility of the cytoplasm (Fritsch and Palmer, unpublished). The amount of the cytoplasmically located SoxY that always gave full reaction with NEM and no reaction with AMS was used as a reference, and as a marker for the total amount of cellular protein applied and for the efficiency of labeling. Only samples standardized in this way were used to compare the labeling. Washed cells of *E. coli* producing SoxY with a hemeagglutinin (HA) tag for detection by antisera were labeled with AMS or NEM, respectively (Figure 3). In the immunoblot

dx.doi.org/10.1021/bi1019995 |*Biochemistry* 2011, 50, 5925–5938

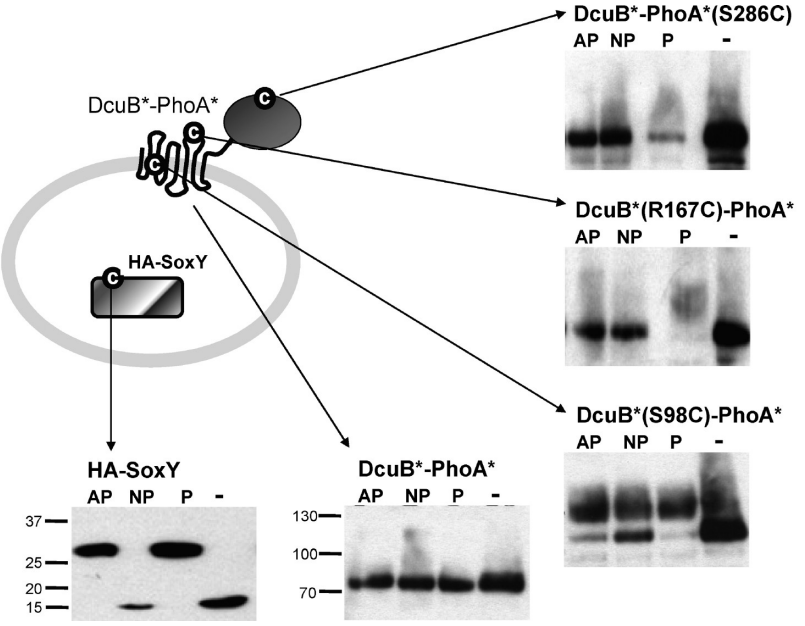

Figure 3. Experimental approach for accessibility studies on DcuB*-PhoA* fusions by AMS/NEM and PEGmal labeling. The scheme in the center shows a cell coproducing cytoplasmic SoxY protein with a hemeagglutinin tag (HA-SoxY) and DcuB*-PhoA* with Cys residues of cytoplasmic, periplasmic, and membrane-integral location. For the experiments *E. coli* C43DE3 containing pMW828 derivatives and pHASoxY were used. The cells were subject to two-step labeling with NEM (N) or AMS (S) in intact cells followed by SDS lysis and reaction with PEGmal (P). (AP) stands for two-step labeling by AMS followed by PEGmal, (NP) for labeling by NEM followed by PEGmal, (P) for one-step labeling with PEGmal (after SDS lysis) and (−) for no labeling. Cell lysate of each sample (10 μg of protein per lane) was subjected to SDS−PAGE, and the fusion protein was detected by immunoblotting with anti-PhoA antisera. The M_r values are shown on the left of the blots for each type of protein. The labeling experiments show the labeling of DcuB*-PhoA*(S286C) (Cys residue in PhoA, periplasmic location, AMS accessible), of DcuB*(R167C)-PhoA* (periplasmic, AMS accessible), of DcuB*(S98C)-PhoA* (no AMS, no NEM accessibility; membrane integral), of DcuB*-PhoA* (Cys-less, no labeling by either reagent), and of HA-SoxY (labeling by NEM, no labeling by AMS).

the HA-SoxY protein was detected as a band of M_r 16 kDa when the protein was denatured in SDS without prior labeling by any of the reagents. When the intact cells were treated first with AMS and in the second step with PEGmal, nearly all of the SoxY protein was labeled by PEGmal as concluded from the mass shift to M_r 28 kDa (Figure 3). In the NEM pretreated cells, only SoxY with the original mass was present, indicating that the protein was labeled by NEM and protected from labeling by PEGmal. In the control, untreated cells were lysed by SDS and then incubated with PEGmal, resulting in PEGmal labeled SoxY. Some experiments of this type showed some SoxY without mass increase, indicating that the reaction of (denatured) SoxY with PEGmal is not always 100%. Altogether the data suggest that the cytoplasmically located HA-SoxY is not accessible to AMS in intact bacteria, whereas NEM has full access, indicating that AMS has no access to cytoplasmic sites. The periplasmically located Cys residue in DcuB*-PhoA*(S286C) on the other hand was not labeled by PEGmal when incubated with either NEM or AMS, demonstrating access of AMS and NEM to PhoA*(S286C) in the intact bacteria.

Neither AMS nor NEM treatment protected efficiently Cys residues that are buried deeply in the membrane like the Cys residue of DcuB*(S98C) from labeling by PEGmal (Figure 3). Thus, DcuB*(S98C) produced similar amounts of DcuB-PEGmal, irrespective of the previous labeling history. Only prior labeling with NEM gave a small fraction of DcuB not labeled by PEGmal, indicating that the Cys residue is accessible to a low extent by NEM. On the other hand, treating the Cys-less mutant DcuB* by AMS/NEM and PEGmal (Figure 3) showed no mass shift for any of the incubation conditions, demonstrating that the labeling is specific for the Cys residues that were introduced in the various proteins.

Overall, it appears that the two-step labeling by AMS/NEM and PEGmal represents a suitable method for differentiating the accessibility of Cys residues that are located at the periplasmic and cytoplasmic sides of the membrane. Under some conditions, even differentiation from residues in the inner membrane is achieved.

Sites in DcuB with Unrestricted Access to AMS from the Outside. Altogether, 39 amino acid residues of DcuB* that were distributed over the entire DcuB protein were singly replaced by Cys residues. All DcuB-Cys variants were functional and supported growth on fumarate. Therefore, the corresponding proteins can be assumed to be correctly inserted into the membrane. These variants of DcuB* carrying single Cys replacements were then used for the differential AMS/NEM plus PEGmal labeling in intact bacteria as described above. Three major classes of Cys residues were detected according to their AMS accessibility. The first class (eight out of 37 residues that were analyzable) represents Cys residues that were almost completely accessible to AMS when the labeling reaction was performed in intact cells under the standardized conditions (Figure 4). The second class of Cys residues (10 residues) was accessible to AMS to a high extent under the standardized conditions, but there was a significant portion of the protein that was not labeled by AMS (Figure 5). The portion of nonreactive DcuB was not decreased by extending the reaction time with AMS. The third class (16 residues) represents residues that were not significantly

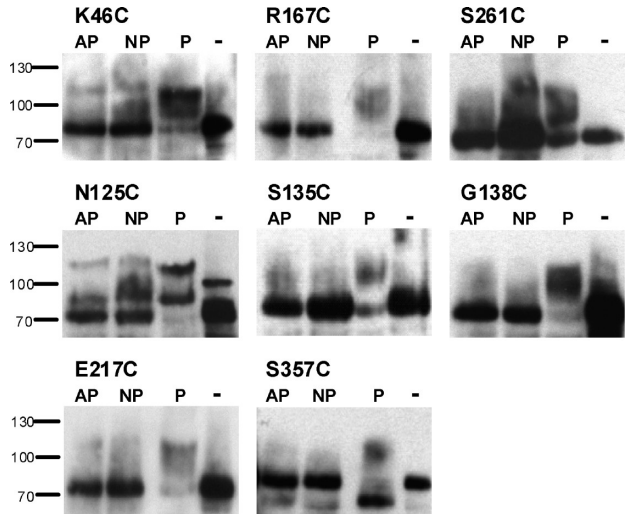

Figure 4. Residues of DcuB accessible to AMS in intact cells. The figure compiles single Cys variants of DcuB* within a DcuB*-PhoA* fusion protein that were accessible to labeling by AMS in intact bacteria. *E. coli* C43DE3 with derivatives of plasmid pMW828 overproducing single cysteine variants of DcuB*-PhoA* and cytoplasmic HA-SoxY was incubated with AMS (A), or NEM (N) or without reagent. After a wash step, the cells were lysed with SDS and labeled with PEGmal (P). Protein of the cell SDS lysate (10 μg of total cell protein per lane) was subject to SDS−PAGE (15% acrylamide) and immunoblotting with anti-PhoA antisera. The size of detected protein bands is labeled on the left side using protein standards.

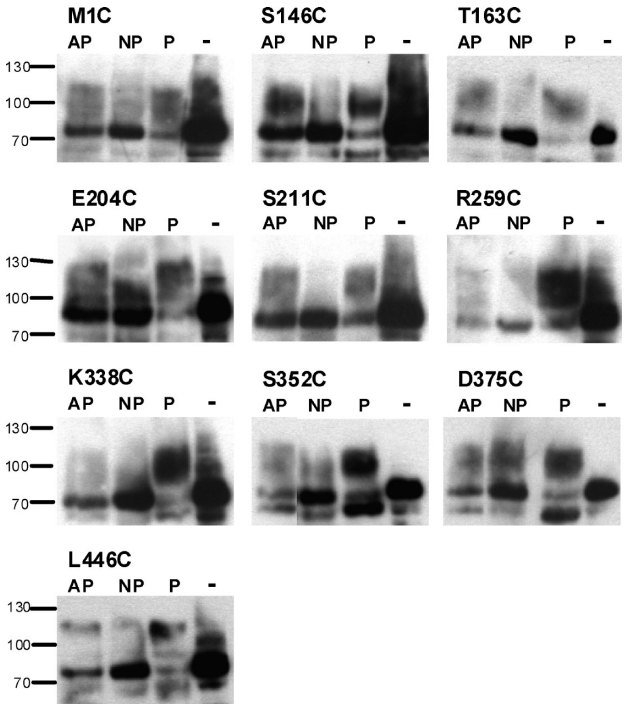

Figure 5. Residues of DcuB with decreased accessibility to AMS in intact cells. The figure compiles single Cys variants of DcuB* in the DcuB*-PhoA* fusion that were accessible to labeling by AMS in intact bacteria but to a significantly lower extent than residues shown in Figure 4. Labeling by AMS was detected by labeling with PEGmal in a second step. For other details see legend to Figure 4. The solubilized cells were applied to SDS−PAGE and immonoblotting, and the DcuB-PhoA fusion protein was detected with anti-PhoA antibodies.

accessible to labeling by AMS, but fully accessible to labeling by NEM (Figure 6A). A small subgroup (3 residues) reacted also with NEM only to low extents (Figure 6B and corresponding text).

Figure 4 gives a summary of labeling reactions for the DcuB Cys^+ variants that were readily accessible to labeling by AMS. Labeling of this type is exemplified by DcuB*(K46C). Labeling by AMS or NEM in the intact cells followed by PEGmal labeling in lysed cells results essentially in one protein band corresponding to unmodified DcuB-PhoA. Only low amounts of PEGmal labeled DcuB with decreased mobility are present. Therefore, the residue K46C is nearly completely accessible to AMS from the outside of the intact cells and consequently protected from PEGmal labeling. The residue is labeled by NEM and protected from PEGmal to a very similar extent as for the AMS experiment.

Similar responses were observed for DcuB* containing a Cys residue in position N125, S135, G138, R167, E217, S261, and S357. Some blots like that for DcuB*(R167C) are complicated in their interpretation due to weak transfer of the PEGmal-labeled protein to the membrane resulting in weak and blurred bands of M_r 90 000 to 115 000. This observation together with the diminished intensity of the band with the original mobility suggests that most of the DcuB derivative has been labeled by PEGmal. The control with SoxY showed that the same amount of cellular proteins has been applied to all samples (not shown). Generally, PEGylated proteins often give blurred and multiple bands, and the mass increase due to PEGylation frequently differs from the predicted values.[34−36] Low blotting efficiency after PEGmal labeling has been reported for other membrane proteins (e.g., ref 34). This response is presumably due to the insertion of the polyethylene glycol chain that affects interaction with SDS and consequently mobility and blotting efficiency of the proteins.

Labeling of DcuB*(N125C) by PEGmal yielded the common M_r 115 000 protein typical for PEGmal labeled DcuB, and an additional band form of DcuB*-PhoA* of $M_r \sim 90\,000$ (Figure 4) which might represent a stable degradation product. The unmodified band of DcuB (apparent M_r about 85 000) disappeared completely, demonstrating that DcuB*(N125C) was completely accessible to PEGmal labeling. The resulting PEGmal labeled DcuB apparently formed two species that differed in mobility for unknown reasons. Bacteria with DcuB*(S357C), after reaction with PEGmal, also retained no DcuB of the original mobility of unmodified DcuB, but the modified forms were different in mobility from most of the other DcuB proteins in Figure 4. For variants DcuB*(N125C) and DcuB*(S357C), the Cys residues were predicted as membrane integral, indicating that labeling in the hydrophobic region may affect folding of the protein and mobility in SDS−PAGE. Overall, the Cys residues of the variant proteins shown in Figure 4 were fully accessible to AMS (and NEM) in intact cells.

Sites in DcuB with Reduced Accessibility for AMS. Ten of the 37 analyzable Cys mutants (Figure 5) were accessible to labeling by AMS and showed high levels of DcuB that were protected from PEGmal after AMS labeling (see sample DcuB*-(S146C) for reference in Figure 5). However, unlike the variants shown in Figure 4, a considerable fraction of the protein was not protected by AMS and was therefore labeled by PEGmal. This is demonstrated by significant levels of the band with decreased mobility and by the relative low amounts of the unmodified (i.e., AMS protected) band. The same type of labeling was found also

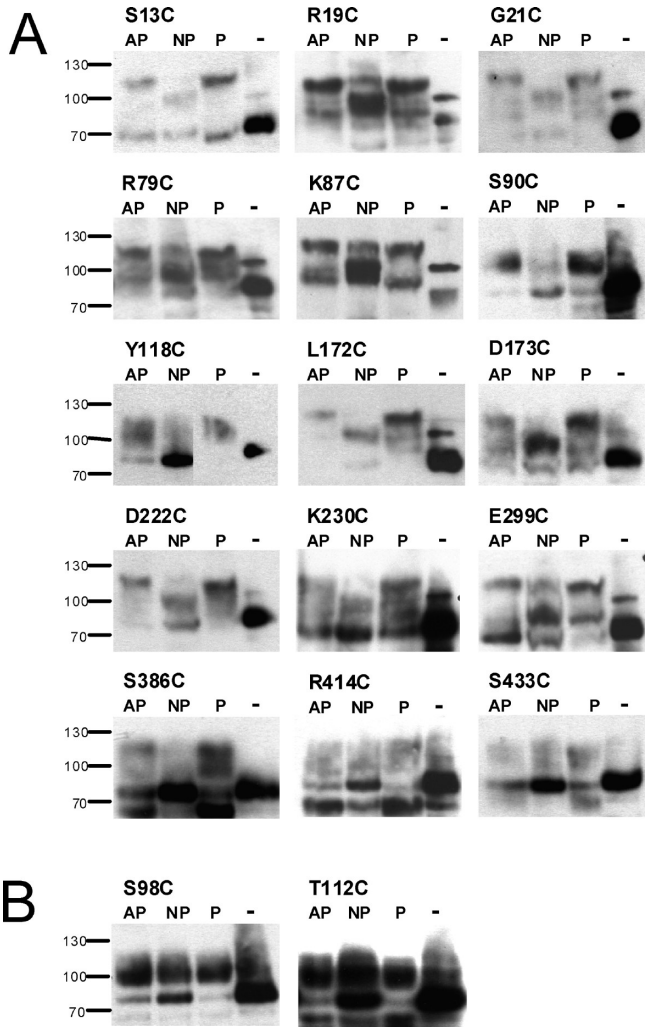

Figure 6. Amino acid residues of DcuB that are not accessible to AMS in intact cells. The figure compiles single Cys variants of DcuB* in the DcuB*-PhoA* fusion that were not accessible to labeling by AMS in intact bacteria but were accessible to labeling by NEM (A). The residues shown in (B) were accessible neither to labeling by AMS nor NEM in intact bacteria. Labeling by AMS or NEM was detected by labeling with PEGmal in second step. For other details see legend to Figure 4. The solubilized cells were applied to SDS−PAGE and immunoblotting with anti-PhoA antibodies.

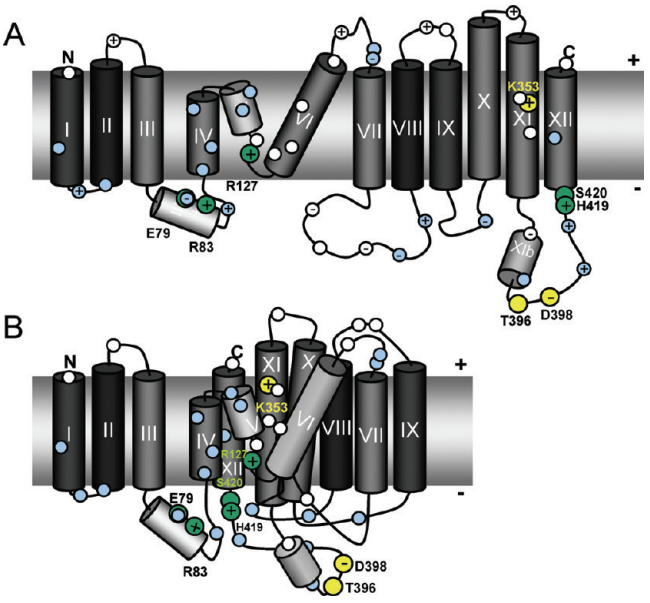

Figure 7. Topology model of DcuB and α-helices based on PhoA/LacZ fusion and AMS accessibility studies. (A) The scheme shows helices I−XII in an extended presentation with the TM helices and their approximate size, and the short helices IV and V that are supposed to form a hairpin structure without passing the membrane. In (B) the central helices that contain AMS or water accessible sites and charged residues (helix VI, IX), and the hairpin loop IV/V are combined in a way that suggests the formation of a water filled transport cavity. The cavity ends in a hypothetical cytoplasmic lid (loop VII−VIII, helix XIb) that contains residues that are accessible in intact bacteria to labeling from the periplasmic side of the membrane. White and blue circles: residues accessible and nonaccessible to periplasmic AMS in intact bacteria: green circles: amino acid residues essential for transport; yellow circles: amino acid residues essential for the function of DcuB as a cosensor of DcuS.

for Cys residues in positions M1C, S146C, T163C, E204C, S211C, D222C, K338C, D375C, and L445C (Figure 5). The portion of PEGmal-reactive DcuB did not decrease when the time of AMS incubation was increased, suggesting a heterogeneous accessibility or reactivity of these forms of DcuB. Nevertheless, a large part of the Cys residues is clearly accessible to AMS from the periplasmic side and has to be regarded as periplasmically accessible, although there is a clear difference to the fully accessible residues shown in Figure 4.

Sites in DcuB with No Accessibility to AMS in Intact Cells. There was a considerable number of Cys residues of the DcuB*-Cys variants that were not accessible to AMS, although the residues were able to react with both NEM and with PEGmal after treating the cells with SDS (Figure 6A). In the immunoblot, the corresponding forms of DcuB showed a mobility after AMS plus PEGmal labeling that was characteristic for DcuB labeled by PEGmal alone. Thus, the major portion of the protein had the mobility of DcuB-PEGmal, and only a small portion the mobility of unmodified DcuB comparable to the sample that was not incubated with labeling reagent. This means the sample was not labeled by AMS. By contrast, incubation with NEM protected DcuB from alkylation by PEGmal. Typical examples for this type of labeling are DcuB*(S13C) or DcuB(K87C) that contain a high fraction of protein with decreased mobility after dual labeling by AMS and PEGmal. The amount of DcuB with the mobility of DcuB-PEGmal is in the same range as in the sample labeled with PEGmal only, whereas the fraction is much lower in the sample labeled first with NEM. A labeling pattern of this type would be expected for residues not accessible to AMS from the outside of the cells. Thus residues C13, R19, G21, R79, K87, S90, Y118, L172, D173, D222, K230, E299, C386, R414, and C433 are apparently not accessible to externally supplied AMS, but to NEM. This type of labeling pattern is characteristic for protein sites not accessible from the extracellular water space.

DcuB* with Cys residues at positions C98 and T112 (Figure 6B) and C104 (not shown) did not react with AMS and showed also low reactivity toward NEM. This indicates a position deeply buried within the hydrophobic space.

DISCUSSION

Topology of DcuB: A 12 TMD Protein. The PhoA and LacZ fusion analysis and the accessibility of engineered Cys residues

dx.doi.org/10.1021/bi1019995 |*Biochemistry* 2011, 50, 5925–5938

indicate that DcuB has 12 transmembrane helices (TMD) with the N- and of the C-terminus located at the periplasmic side of the membrane. The topology of TMDs I to III and VII to XII is consistent with predictions of transmembrane helices by hydropathy plots. TMD I was predicted by the TMHMM server with low probability, but the membrane integration of the DcuB(R19) and DcuB(G21) fusions and the labeling of DcuB at residue 1 by AMS in intact cells strongly indicate the presence of the helix and the periplasmic location of Met(1). For the intermediate region (TMDs IV−VI in Figures S1 and 7) membrane integral α-helical domains are predicted but the topological arrangement was not clear from the PhoA and LacZ studies, and the region showed residues with periplasmic and cytoplasmic accessibilities that did not fit in a conventional arrangement of transmembrane helices (see Figure 7A). The PSIPRED prediction program in combination with the topology studies indicates the presence of α-helical hairpin structures that do not completely span the membrane. Transmembrane helices require a minimal number of 18 amino acid residues to cross a phospholipid bilayer,[37] but for helices IV and V only a maximum of 12−15 residues is predicted by the PSIPRED server. On the other hand, TMD VI, X, and XI with predicted sizes of about 29 or 30 amino acid residues are very long (Figure 7). In addition, three α-helices were predicted for the cytosolic loop regions III−IV, VII−VIII (not shown in Figure 7), and XI-XII. The cytoplasmic loop XI−XII contains in addition three predicted β-sheet structures.

Sites with Unexpected AMS Accessibility: Topological and Functional Implications. The studies of AMS accessibility confirmed the overall topology of DcuB and provided additional clues to DcuB topology and function (Figure 7). DcuB variants containing single Cys residues were functional in transport and regulation, supporting the functional relevance of the data. Most of the periplasmic sites according to the model of Figure 7 were accessible to labeling by AMS as expected. The lack of accessibility of residues L172 and D173 could be due to the proximity to the membrane or protection by steric hindrance. AMS is a flat molecule with dimensions of about 7 × 18 Å (Chem3DUltra, www.cambridgesoft.com) and not able to pass the membrane and to react with cytoplasmic thiol groups as documented with the SoxY protein in intact cells. However, several amino acid residues of DcuB with a clear cytoplasmic location (E204, E217, S211, D222 in loop VII−VIII and D375 in loop XI-XII) or a location within the membrane (N125, S135, G138, S146, and S357) were at least partly labeled by AMS (Figure 7). In particular, the loop VII−VIII contains AMS accessible residues, although a cytoplasmic location was clearly demonstrated by the PhoA/LacZ reporter fusions and the topology of the adjacent TMDs VII and VIII. Moreover, the loop is saturated by positively charged amino acid residues and therefore cytoplasmic according to the positive-inside rule.[38] The same problem arises for D375 of loop XI−XII that is labeled by AMS in intact bacteria. The loop has a cytoplasmic location according to PhoA/LacZ reporter fusions and the AMS protected residues S386 and R414 of the loop.

Maleimides require the Cys residues in the deprotonated thiolate form in order to react, and the deprotonation occurs preferentially by water. Therefore, the reaction of apparently membrane integral residues with AMS suggests the presence of a water-filled cavity in order to allow access and reaction. Helices VI and XI and loop V−VI are suggested to form the water filled cavity for fumarate/succinate translocation due to the large number of AMS accessible residues. Helix VI apparently plays a central role; the AMS accessible amino acid residues S135, G138, and S146 are all predicted to be located on one side of helix VI. The cytoplasmic loop VII−VIII, and possibly also loop XI−XII might form a cytoplasmic lid to seal the cavity from the cytoplasmic side. A hypothetical model for the arrangement of the TMDs and loops of DcuB is shown in Figure 7B.

Membrane impermeable maleimide derivatives are able to react with cysteine thiolates at positions five to six residues within the membrane of a TMD (counting from membrane surface). The cysteinyl side chain is able to bridge the corresponding distance.[39] A water-filled cavity allows reaction of AMS in the membrane integral layer with residues more deeply embedded and potentially also with residues close to the cytoplasmic side of a waterfilled channel. This assumption may provide an explanation for reaction of the "cytoplasmic" residues E204, E217, S211, D222, and D375, although AMS was not able to pass the membrane. This finding strongly supports the presence of a water-filled cavity that is in contact to the cytoplasmic loops in that region. This arrangement is reminiscent of the mitochondrial ADP/ATP carrier that forms a deep central cavity.[40,41] The cavity carries the site for adenine nucleotide exchange and is shut off from the matrix by a lid forming the bottom of the cavity. Open transport cavities have also been demonstrated for the structurally well-characterized transporters LacY, GlpT, and EmrD.[42−44]

Accordingly, TMDs VI, XI, and loops V−VI are suggested to contribute to the transport channel of DcuB (Figure 7B). TMD X contains charged amino acid residues, and TMD XII contains the transport-relevant sites H419 and S420.[12] Part of the cytoplasmic loop VII−VIII and the soluble α-helix XIb apparently are supposed to seal the waterfilled transport cavity. In the arrangement suggested in Figure 7B, the hydrophobic helices I, II, VIII, and XI form the contact of the transport channel to the surrounding membrane.

DcuB versus DcuA. DcuA and DcuB differ significantly in their topology despite being members of the same family of permeases (Figure 8). The transmembrane topology of DcuA is based on the study by Golby et al.[23] and on the present study. DcuA and DcuB consist of 10 and 12 TMDs, respectively. Helices I_B to IV_B and $VIII_B$ to XI_B of DcuB have direct counterparts in DcuA, whereas helices V_B and VII_B of DcuB have not. The major differences lie in the regions corresponding to the water filled cavity and the C-terminus of DcuB following XI_B (Figure 8). The C-terminus of DcuB is characterized by a large cytoplasmic loop followed by TM XII_B with an in−out arrangement. The final TMX_A of DcuA, on the other hand, is followed by a long periplasmic loop. Overall, the lack of the two TMDs in DcuA is explained by differences in the formation of TMDs in corresponding regions.

The structural and topological differences between DcuB and DcuA might be important for the observed functional differences. Both transporters are able to catalyze antiport, uptake, and efflux of C_4-dicarboxylates.[4,5] The physiological role of DcuB, however, is an electroneutral fumarate^{2-}/succinate^{2-} antiport, whereas DcuA is assumed to function as a back-up carrier for uptake and antiport. The topology model locates two sensory competent residues of DcuB (T394 and D398) in the DcuB-specific large cytoplasmic loop XI-XII_B, and this loop might be important for the function of DcuB in cosensing and interaction with DcuS.[12] The third sensory competent residue (K353) in TMD XI is part of the supposed water-filled cavity (Figure 7). Knowing the topology of the sensory competent residues will be

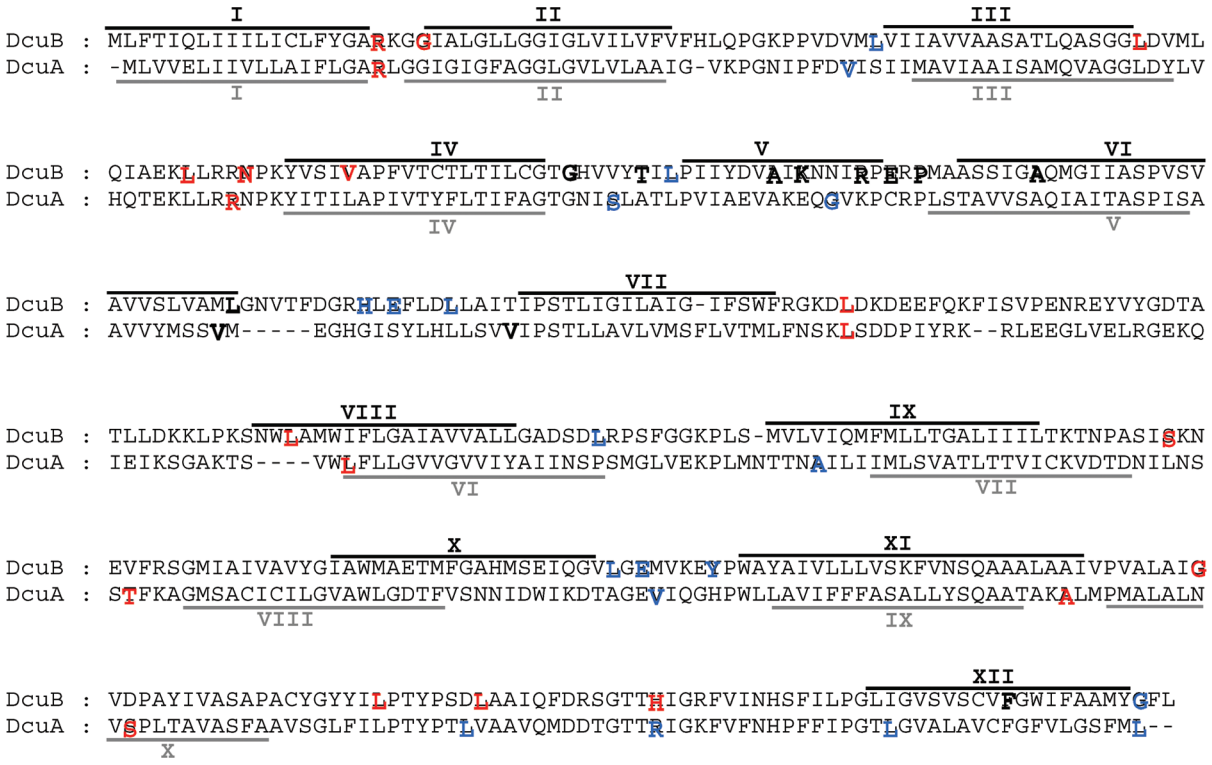

Figure 8. Comparison of the topology model for DcuB and DcuA: Allocation of the predicted TMDs to the sequences of DcuB and DcuA. Topology models for DcuB and DcuA are based on the topology of the hydrophilic loops (see Figures 2 and S1) and the prediction of hydrophobic TM helices. The PhoA and LacZ junction sites are labeled by circles. The topology of DcuA is similar to the topology model of Golby et al.[23] The location of the TMDs (I−XII of DcuB and I−X of DcuA) is aligned to the sequences of the proteins and shown by the lines on the top or below the sequences (red: cytoplasmic; blue: periplasmic location; black: no clear evidence). The amino acid residues of DcuB and DcuA at the PhoA and LacZ fusion sites (last residues of DcuB and DcuA, respectively) are printed in bold.

important for understanding the role of DcuB in controlling DcuS function.

Secondary Transporters That Serve As Models for DcuB Topology. Cys residues in TMDs of other permeases are known for their accessibility to bulky thiol reagents when they are located in a water-filled channel. In the multidrug ABC transporter LmrA of *Lactococcus lactis* Cys residues of a predicted transmembrane helix reacted with fluorescein-5-maleimide.[45] The periodicity of maleimide accessibility to every third or fourth residue of the helix indicated the presence of a water-filled cavity and the side of exposure to water, and the exposure of the everted side to the lipid environment or the neighboring lipophilic α-helices. A similar accessibility pattern was shown for residues of the transport sites of the Na^+/proline transporter PutP[46] and of the osmoprotectant transporter ProP.[47] As described before, the presence of a large water filled cavity ending in a structure that seals the cavity to the other side of the membrane is well-known from the mitochondrial ADP/ATP translocator.[40,41]

The topology model for DcuB suggests several uncommon structural features (Figure 7) like long and tilted transmembrane helices (TM VI, X, XI), a helical hair pin (TM IV and V), and hydrophilic or charged membrane integral elements (TM VI, XI, and part of V). Structures of this type have been determined for several secondary transporters.[42,45,49] Thus, kinked, tilted and water-accessible TM helices, and helical hairpins play an important role in forming the water-filled cavity and binding and translocating the substrate. The glutamate transporter Glt_{Ph} from *Pyrococcus horikoshi* contains all the structural elements discussed here for DcuB (see refs 48, 50−52). Glt_{Ph} and DcuB are members of different transporter families, but they share similar substrates, C_4-dicarboxylates including L-aspartate for DcuB and glutamate for Glt_{Ph}. This demonstrated the usefulness of the methods employed here to obtain topology and structural information for membrane proteins that are not accessible to direct structural analysis.

Up to 70% of the membrane proteins with 12 TMDs have been predicted by a bioinformatic study to be composed of internal structural repeats.[53] Such an internal repeat structure is apparently absent in DcuB as indicated by the noncentral location of the supposed transport cavity, the nonsymmetric arrangement of TMDs and of the large cyoplasmic loops (compare Figure 7). There is also a functional asymmetry as indicated by the location of mutations inhibiting transport in the (noncentral) transport-cavity and the mutations deficient in regulation located close to the C-terminus. The structural elements and their arrangement is reminiscent of the glutamate transporter Glt_{Ph} of *Pyrococcus horikoshii*. The transporter lacks internal repeats and the protein is arranged as a membrane-integral homotrimer.[48]

■ ASSOCIATED CONTENT

Supporting Information. The topology studies on DcuA (PhoA and LacZ fusions) and topology comparison between DcuB and DcuA (Figure S1). Tables S1−S3 listing the complete selection of plasmids and of the oligonucleotides used for gene

amplification and for mutation are included. This material is available free of charge via the Internet at http://pubs.acs.org.

AUTHOR INFORMATION

Corresponding Author

*Phone +06131-3923550. Fax +06135-3922695. E-mail: unden@uni-mainz.de.

Funding Sources

The work was supported by grants of Deutsche Forschungsgemeinschaft (DFG) to G.U. and by a travel grant of Deutscher Akademischer Austauschdienst (DAAD) to J.B. M.J.F. is supported by a Ph.D. studentship from the BBSRC.

ACKNOWLEDGMENT

We are grateful to Dr. B. Berks for supplying us with the *soxY* gene via plasmid pVS005, Dr. H. Jung for plasmids pT7-5-putP-lacZ and pT7-5-putP-phoA, and J. Witan (Mainz) for helpful comments on the manuscript.

ABBREVIATIONS USED

AMS, 4-acetamido-4′-maleimidylstilbene-2,2′-disulfonate; BlaM, β-lactamase; DcuA, C4-dicarboxylate uptake transporter A; DcuB, C4-dicarboxylate uptake transporter B; DcuS, C4-dicarboxylate uptake sensor; DMSO, dimethyl sulfoxide; NEM, *N*-ethylmaleimide; ONPG, *o*-nitrophenyl galactoside; PEGmal, polyethylene-glycol-maleimide; PNPP, *p*-nitrophenyl phosphate; TMD, transmembrane domain; TM, transmembrane helix

REFERENCES

(1) Unden, G., Kleefeld, A. (2004) C_4-Dicarboxylate degradation in aerobic and anaerobic growth. Module 3.4.5, in *EcoSal — Escherichia coli and Salmonella: Cellular and Molecular Biology* (Curtiss, R., III, Ed.) ASM Press, Washington, DC, http://www.ecosal.org.

(2) Yurgel, S. N., and Kahn, M. L. (2004) Dicarboxylate transport by rhizobia. *FEMS Microbiol. Rev. 28*, 489–501.

(3) Janausch, I. G., Zientz, E., Tran, Q. H., Kröger, A., and Unden, G. (2002) C_4-dicarboxylate carriers and sensors in bacteria. *Biochim. Biophys. Acta 1553*, 39–56.

(4) Six, S., Andrews, S. C., Unden, G., and Guest, J. R. (1994) *Escherichia coli* possesses two homologous anaerobic C4-dicarboxylate membrane transporters (DcuA and DcuB) distinct from the aerobic dicarboxylate transport system (Dct). *J. Bacteriol. 176*, 6470–6478.

(5) Engel, P, Krämer, R., and Unden, G. (1994) Transport of C_4-dicarboxylates by anaerobically grown *Escherichia coli*: energetics and mechanism of exchange, uptake and efflux. *Eur. J. Biochem. 222*, 605–614.

(6) Golby, P., Davies, S., Kelly, D. J., Guest, J. R., and Andrews, S. C. (1999) Identification and characterisation of a two-component sensor-kinase and response-regulator system (DcuS-DcuR) controlling gene expression in response to C_4-dicarboxylates in *Escherichia coli*. *J. Bacteriol. 181*, 1238–1248.

(7) Davies, S., Golby, P., Omrani, D., Broad, S. A., Harrington, V. L., Guest, J. R., Kelly, D. J., and Andrews, S. C. (1999) Inactivation and regulation of the aerobic C_4-dicarboxylate transport (*dctA*) gene of *Escherichia coli*. *J. Bacteriol. 181*, 5624–5635.

(8) Zientz, E., Bongaerts, J., and Unden, G. (1998) Fumarate regulation of gene expression in *Escherichia coli* by the DcuSR (*dcuSR* genes) two-component regulatory system. *J. Bacteriol. 180*, 5421–5425.

(9) Zientz, E., Six, S., and Unden, G. (1996) Identification of a third secondary carrier (DcuC) for anaerobic C_4-dicarboxylate transport in *Escherichia coli*: role of the three Dcu carriers in uptake and exchange. *J. Bacteriol. 178*, 7241–7247.

(10) Golby, P., Kelly, D. J., Guest, J. R., and Andrews, S. C. (1998) Transcriptional regulation and organization of the *dcuA* and *dcuB* genes, encoding homologous anaerobic C_4-dicarboxylate transporters in *Escherichia coli*. *J. Bacteriol. 180*, 6586–6596.

(11) Zientz, E., Janausch, I. G., Six, S., and Unden, G. (1999) Function of DcuC as the C_4-dicarboxylate carrier during glucose fermentation by *Escherichia coli*. *J. Bacteriol. 181*, 3716–3720.

(12) Kleefeld, A., Ackermann, B., Bauer, J., Krämer, J., and Unden, G. (2009) The fumarate/succinate antiporter DcuB of *Escherichia coli* is a bifunctional protein with sites for regulation of DcuS-dependent gene expression. *J. Biol. Chem. 284*, 265–275.

(13) Kneuper, H., Janausch, I. G., Vijayan, V, Zweckstetter, M., Bock, V., Griesinger, C., and Unden, G. (2005) The Nature of the stimulus and the fumarate binding site of the fumarate sensor DcuS of *Escherichia coli*. *J. Biol. Chem. 280*, 20596–20603.

(14) Scheu, P. D., Kim, O. B., Griesinger, C., and Unden, G. (2010) Sensing by the membrane-bound sensor kinase DcuS: exogenous versus endogenous sensing of C4-dicarboxylates in bacteria. *Future Microbiol. 5*, 1383–1402.

(15) Pappalardo, L., Janausch, I. G., Vijayan, V., Zientz, E., Junker, J., Peti, W., Zweckstetter, M., Unden, G., and Griesinger, C. (2003) The NMR structure of the sensory domain of the membranous two-component fumarate sensor (histidine protein kinase) DcuS of *Escherichia coli*. *J. Biol. Chem. 278*, 39185–39188.

(16) Cheung, J., and Hendrickson, W. A. (2008) Crystal structures of C_4-dicarboxylate ligand complexes with sensor domains of histidine kinases DcuS and DctB. *J. Biol. Chem. 283*, 30256–30265.

(17) Mascher, T., Helmann, J. D., and Unden, G. (2006) Stimulus perception in bacterial signal transducing histidine kinases. *Microbiol. Mol. Biol. Rev. 70*, 910–938.

(18) Etzkorn, M., Kneuper, H., Dünnwald, P., Vijayan, V., Krämer, J., Griesinger, C., Becker, S., Unden, G., and Baldus, M. (2008) Plasticity of the PAS domain and a potential role for signal transduction in the histidine kinase DcuS. *Nat. Struct. Mol. Biol. 15*, 1031–1039.

(19) Tetsch, L., and Jung, K. (2009) The regulatory interplay between membrane-integrated sensors and transport proreins in bacteria. *Mol. Microbiol. 73*, 982–991.

(20) Manoil, C., Boyd, D., and Beckwith, J. (1988) Molecular genetic analysis of membrane protein topology. *Trends Genet. 4*, 223–226.

(21) Hagting, A., Kunji, E. R., Leenhouts, K. J., Poolman, B., and Konings, W. N. (1994) The Di-and Tripeptide Protein of *Lactococcus lactis*. *J. Biol. Chem. 269*, 11391–11399.

(22) Long, J. C., Wang, S., and Vik, S. B. (1998) Membrane topology of subunit a of the F1F0 ATP synthase as determined by labeling of unique cysteine residues. *J. Biol. Chem. 273*, 16235–16240.

(23) Golby, P., Kelly, D. J., Guest, J. R., and Andrews, S. C. (1998) Topological analysis of DcuA, an anaerobic C_4-dicarboxylate transporter of *Escherichia coli*. *J. Bacteriol. 180*, 4821–4827.

(24) Sambrook, J., Russel, D. W. (2001) *Molecular cloning: A Laboratory Manual*, 3rd ed., Vol. 3, Cold Spring Harbor Laboratory Press, New York.

(25) Dower, W. J., Miller, J. F., and Ragsdale, C. W. (1988) High efficiency transformation of *E. coli* by high voltage electroporation. *Nucleic Acids Res. 16*, 6127–6145.

(26) Krämer, J., Fischer, J., Zientz, E., Vijayan, V., Griesinger, C., Lupas, A., and Unden, G. (2007) Citrate sensing by the C_4-dicarboxylate/citrate sensor kinase DcuS of *Escherichia coli*: binding site and conversion of DcuS to a C_4-dicarboxylate- or citrate-specific sensor. *J. Bacteriol. 189*, 4290–4298.

(27) Guzman, L.-M., Belin, D., Carson, M. J., and Beckwith, J. (1995) Tight regulation, modulation and high-level expression by vectors containing the arabinose P_{BAD} promotor. *J. Bacteriol. 177*, 4121–4130.

(28) Jung, H., Ruebenhagen, R., Tebbe, S., Leifker, K., Tholema, N., Quick, M., and Schmid, R. (1998) Topology of the Na^+/proline transporter of *Escherichia coli*. *J. Biol. Chem. 273*, 26400–26407.

(29) Michaelis, S., Guarente, L., and Beckwith, J. (1983) In vitro construction and characterization of *phoA-lacZ* gene fusions in *Escherichia coli*. *J. Bacteriol. 154*, 356–365.

(30) Calamia, J., and Manoil, C. (1990) Lac permease of *Escherichia coli:* topology and sequence elements promoting membrane insertion. *Proc. Natl. Acad. Sci. U. S. A. 87*, 4937–4941.

(31) Miller, J. H. (1992) *A Short Course in Bacterial Genetics*, Cold Spring Harbour Laboratory Press, New York.

(32) Bogdanov, M., Zhang, W., Xie, J., and Dowhan, W. (2005) Transmembrane protein topology mapping by the substituted cysteine accessibility method (SCAM): application to lipid-specific membrane protein topogenesis. *Methods 36*, 148–171.

(33) Kimura-Someya, T., Iwaki, S., and Yamaguchi, A. (1998) Site-directed chemical modification of cysteine-scanning mutants as to transmembrane segment II and its flanking regions of the Tn10-encoded metal-tetracycline/H^+ antiporter reveals a transmembrane water-filled channel. *J. Biol. Chem. 273*, 32806–32811.

(34) Maegawa, S., Koide, K., Ito, K., and Akiyama, Y. (2007) The intramembrane active site of GlpG, an E. coli rhomboid protease, is accessible to water and hydrolyses an extramembrane peptide bond of substrates. *Mol. Microbiol. 64*, 435–447.

(35) Lu, J., and Deutsch, C. (2001) PEGylation: a method for assessing topological accessibilities in Kv1.3. *Biochemistry 40*, 13288–13301.

(36) Zheng, C., Ma, G., and Su, Z. (2007) Native PAGE eliminates the problem of PEG-SDS interaction in SDS-PAGE and provides an alternative to HPLC in characterization of protein PEGylation. *Electrophoresis 28*, 2801–2807.

(37) White, S. H., Ladokhin, A. S., Jayasinghe, S., and Hristova, K. (2001) How membranes shape protein structure. *J. Biol. Chem. 276*, 32395–32398.

(38) Heijne von, G. (1986) The distribution of positively charged residues in bacterial inner membrane proteins correlates with the transmembrane topology. *EMBO J. 5*, 3021–3027.

(39) Fu, D., and Maloney, P. C. (1998) Structure-function relationships in OxlT, the oxalate/formate transporter of *Oxalobacter formigenes*. Topological features of transmembrane helix 11 as visualized by site-directed fluorescÿ abellingling. *J. Biol. Chem. 273*, 17962–17967.

(40) Pebay-Peyroula, E., Dahout-Gonzalez, C., Kahn, R., Trézéguet, V., Lauquin, G. J. M., and Brandolin, G. (2003) Structure of mitochondrial ADP/ATP carrier in complex with caroxyatractyloside. *Nature 426*, 39–44.

(41) Pebay-Peyroula, E., and Brandolin, G. (2004) Nucleotide exchange in mitochondria: insight at a molecular level. *Curr. Opin. Struct. Biol. 14*, 420–425.

(42) Abramson, J., Smirnova, I., Kasho, V., Verner, G., Kaback, H. R., and Iwata, S. (2003) Structure and mechanism of the lactose permease of *Escherichia coli*. *Science 301*, 610–615.

(43) Huang, Y., Lemieux, M. J., Song, J., Auer, M., and Wang, D. N. (2003) Structure and mechanism of the glycerol-3-phosphate transporter from *Escherichia coli*. *Science 301*, 616–620.

(44) Yin, Y., He, X., Szewczyk, P., and Nguyen, T. (2006) Structure of the multidrug transporter EmrD from *Escherichia coli*. *Science 312*, 741–744.

(45) Poelarends, G. J., and Konings, W. N. (2002) The transmembrane domains of the ABC multidrug transporter LmrA form a cytoplasmic exposed, aqueous chamber within the membrane. *J. Biol. Chem. 277*, 42891–42898.

(46) Pirch, T., Landmeier, S., and Jung, H. (2003) Transmembrane domain II of the Na+/proline transporter PutP of *Escherichia coli* forms part of a conformationally flexible, cytoplasmic exposed aqueous cavity within the membrane. *J. Biol. Chem. 278*, 42942–42949.

(47) Liu, F., Culham, D. E., Vernikovska, Y. I., Keates, R. A., Boggs, J. M., and Wood, J. M. (2007) Structure and function of transmembrane segment XII in osmosensor and osmoprotectant transporter ProP of *Escherichia coli*. *Biochemistry 46*, 5647–5655.

(48) Yernool, D., Boudker, O., Jin, Y., and Gouaux, E. (2004) Structure of a glutamate transporter homologue from *Pyrococcus horikoshii*. *Nature 431*, 811–818.

(49) Yamashita, A, Singh, S. K., Kawate, T., Jin, Y., and Gouaux, E. (2005) Crystal structure of a bacterial homologue of Na^+ Cl^--dependent neurotransmitter transporters. *Nature 437*, 215–223.

(50) Boudker, O., Ryan, R. M., Yernool, D., Shimamoto, K., and Gouaux, E. (2007) Coupling substrate and ion binding to extracellular gate of a sodium-dependent aspartate transporter. *Nature 445*, 387–393.

(51) Reyes, N., Ginter, C., and Boudker, O. (2009) Transport mechanism of a bacterial homologue of glutamate transporters. *Nature 462*, 880–885.

(52) Boudker, O., and Verdon, G. (2010) Structural perspectives on secondary active transporters. *Trends Pharmacol. Sci. 31*, 418–426.

(53) Hennerdal, A., Lindahl, E., and Elefsson, A. (2010) Internal duplications in α-helical membrane topologies are common but the nonduplicated forms are rare. *Protein Sci. 19*, 2305–2318.

(54) Bryson, K., McGuffin, L. J., Marsden, R. L., Ward, J. J., Sodhi, J. S., and Jones, D. T. (2005) Protein structure prediction servers at University College London. *Nucleic Acids Res. 33*, W36–W38(Web Server Issue).

(55) Kyte, J., and Doolittle, R. F. (1982) A simple method for displaying the hydrophatic character of a protein. *J. Mol. Biol. 157*, 105–132.

(56) Miroux, B., and Walker, J. E. (1996) Overproduction of Proteins in *Escherichia coli*: mutant hosts that allow syntheses of some membrane proteins and globular proteins at high levels. *J. Mol. Biol. 260*, 289–298.

(57) Silhavy, T. J., Berman, M. L., Enquist, L. W. (1984) *Experiments with Gene Fusions*, Cold Spring Harbor Laboratory Press, New York.

(58) Heeb, S., Itoh, Y., Nishijyo, T., Schnider, U., Keel, C., Wade, J., Walsh, U., O'Gara, F., and Haas, D. (2000) Small, stable shuttle vectors based on the minimal pVS1 replicon for use in gram-negative, plant-associated bacteria. *Mol. Plant-Microbe Interact. 13*, 232–237.